



Contents lists available at ScienceDirect

Arabian Journal of Chemistry

journal homepage: www.ksu.edu.sa

Chemical change and mechanism of *Milletia speciosa* with sulfur fumigation by UHPLC–QTOF–MS/MS

Jianguang Zhang^{a,b,1}, Lili He^{c,1}, Junjun Wang^a, Li Yang^a, Ming Chen^b, Zichang Liang^b, Zhifeng Zhang^{a,*}

^a Tibetan Plateau Ethnic Medicinal Resources Protection and Utilization Key Laboratory of National Ethnic Affairs Commission of the People's Republic of China, Southwest Minzu University, Chengdu 610041, China

^b Qin Zhou Provincial Health School, Qinzhou 53500, China

^c National Engineering Institute for the Research and Development of Endangered Medicinal Resources in Southwest China, Guangxi Botanical Garden of Medicinal Plants, Nanning, Guangxi 530005, China

ARTICLE INFO

Keywords:

Milletia speciosa
UHPLC–QTOF–MS/MS
Multivariate analysis
Sulfur fumigation
Chemical transformation

ABSTRACT

Milletia speciosa Champ. (MSCP), which is distributed and used in Southern China, is often sulfur-fumigated during postharvest handling to prevent insects and molds. In the present study, a comprehensive strategy was proposed by using ultrahigh-performance liquid chromatography-quadrupole/time-of-flight mass spectrometry (UHPLC–QTOF–MS/MS) with multivariate analysis to rapidly identify potential chemical sulfur-fumigated MSCP (SF-MSCP) samples, discover chemical transformation mechanisms and control the quality of SF-MSCP. Eighty-six compounds were tentatively assigned, and ten compounds were screened out as potential markers. Moreover, the chemical transformation mechanism was deduced by hydrolysis, esterification and dehydration reactions that occurred during the sulfur-fumigated process. The developed method was successfully applied to predict 16 commercial MSCP samples, and 9 samples were found to contain sulfur compounds, ranging in sulfur residues from 100 to 310 mg/kg. These research outcomes can not only be used to distinguish the nonfumigated MSCP from SF-MSCP by chemical markers but also provide a chemical basis for further comprehensive investigating in-depth safety and functional evaluations of SF-MSCP.

1. Introduction

Milletia speciosa Champ. (MSCP) is called Niudali, a famous edible herb medicine that is widely distributed in Guangxi, Guangdong and Hainan Provinces of China (Wang et al., 2021). Phytochemical analysis has shown that MSCP mainly contains terpenoids, flavonoids, alkaloids, polysaccharides, phenylpropanoids and so on (Zhao et al., 2017; Wang et al., 2021). These constituents have been reported as the primary active ingredients associated with MSCP pharmacological activity, such as anti-fatigue (Zhao et al., 2015), enhancing immunomodulatory (Huang et al., 2020), antioxidative (Huang, Zhong, & Long, 2022), and anti-depressive activities (Chi et al., 2021). The root of MSCP has been used in Chinese medicine for the treatment of chronic bronchitis, coughing, rheumatic arthritis and kidney-deficiency syndrome (Zhao et al., 2017). In folk medicine, MSCP is commonly decocted with pig

bone due to its health benefits, including boosting the immune system, reducing inflammation and recovering strength.

In southern China, the humid climate causes the medicine to easily mold, which may spoil medicinal materials during storage. Additionally, some medicinal materials may be damaged by insects during storage. To maintain a humid climate and better color, sulfur is often used to fumigate fresh MSCP during the postharvest handling process, which bleaches the color of materials and maintains a good appearance. In recent decades, sulfur fumigation with high efficiency, simple operation, reliability and low cost has been widely used for postharvest handling of some foods and medicinal herbs to guard against insects, maintain color and freshness, protect moisture and obtain a longer storage life (Jiang, Huang, Zheng, & Chen, 2013). However, the quality of the herbal medicine may change, and sulfur dioxide (SO₂) can remain in it. Residual SO₂ has been regarded as the major factor that affects the quality

Peer review under responsibility of King Saud University.

* Corresponding author at: 15# Southwest Minzu University, No.16, South 4th Section 1st Ring Road, Chengdu 610041, Sichuan, China.

E-mail address: zfzhang@swun.edu.cn (Z. Zhang).

¹ These authors contributed equally to this work.

<https://doi.org/10.1016/j.arabjc.2023.105509>

Received 13 May 2023; Accepted 29 November 2023

Available online 1 December 2023

1878-5352/© 2023 The Author(s). Published by Elsevier B.V. on behalf of King Saud University. This is an open access article under the CC BY-NC-ND license (<http://creativecommons.org/licenses/by-nc-nd/4.0/>).

Table 1
Samples of MSCP analyzed in this study.

No. of sample	Description	Collecting location	The residual sulfur(mg/kg)	Characteristic markers (peak number)
NF-1	Non-fumigated sample	Qinzhou, Guangxi	–	
SF-1	sulfur-fumigated sample	Qinzhou, Guangxi	245	1, 2, 12, 14, 63, 64, 65, 66
NF-2	Non-fumigated sample	Qinzhou, Guangxi	–	
SF-2	sulfur-fumigated sample	Qinzhou, Guangxi	120	2, 11, 12, 38,63, 64, 65
NF-3	Non-fumigated sample	Yulin, Guangxi	–	
SF-3	sulfur-fumigated sample	Yulin, Guangxi	330	1, 2, 11, 12, 14, 38,63, 64, 65, 66
NF-4	Non-fumigated sample	Yulin, Guangxi	–	
SF-4	sulfur-fumigated sample	Yulin, Guangxi	342	2, 11, 12, 14, 38,63, 64, 65, 66
NF-5	Non-fumigated sample	Shangsi, Guangxi	–	
SF-5	sulfur-fumigated sample	Shangsi, Guangxi	440	1, 2, 11, 12, 14, 38,63, 64, 65, 66
NF-6	Non-fumigated sample	Shangsi, Guangxi	–	
SF-6	sulfur-fumigated sample	Shangsi, Guangxi	220	2, 12, 14, 38,63, 66
NF-7	Non-fumigated sample	Nanning, Guangxi	–	
SF-7	sulfur-fumigated sample	Nanning, Guangxi	630	1, 2, 12, 14, 38,63, 64, 65, 66
NF-8	Non-fumigated sample	Nanning, Guangxi	–	
SF-8	sulfur-fumigated sample	Nanning, Guangxi	540	2, 12, 14, 38,63, 64, 65, 66
NF-9	Non-fumigated sample	Qinzhou, Guangxi	–	
SF-9	sulfur-fumigated sample	Qinzhou, Guangxi	420	1, 2, 11, 12, 38,63, 64, 65, 66
NF-10	Non-fumigated sample	Shangsi, Guangxi	–	
S1	Commercial sample	Yulin, Guangxi	–	
S2	Commercial sample	Yulin, Guangxi	–	
S3	Commercial sample	Yulin, Guangxi	100	1, 14, 38,63, 64, 65
S4	Commercial sample	Yulin, Guangxi	138	2, 12, 14, 38,63, 64, 65, 66
S5	Commercial sample	Yulin, Guangxi	225	1,2, 11, 14, 38,63, 64, 65, 66
S6	Commercial sample	Hehuqchi, Chengdu	–	
S7	Commercial sample	Hehuqchi, Chengdu	210	2, 12, 38,63, 64,
S8	Commercial sample	Hehuqchi, Chengdu	–	
S9	Commercial sample	Hehuqchi, Chengdu	125	2, 12, 63, 64, 65, 66
S10	Commercial sample	Bozhou, Anhui	–	
S11	Commercial sample	Bozhou, Anhui	–	
S12	Commercial sample	Bozhou, Anhui	310	2, 11, 12, 38,63, 64, 65

Table 1 (continued)

No. of sample	Description	Collecting location	The residual sulfur(mg/kg)	Characteristic markers (peak number)
S13	Commercial sample	Qinzhou, Guangxi	–	
S14	Commercial sample	Qinzhou, Guangxi	140	2, 11, 38,63, 64, 66
S15	Commercial sample	Nanning, Guangxi	160	1, 12, 14, 63, 64, 65
S16	Commercial sample	Nanning, Guangxi	180	2, 11, 12, 63, 64, 65, 66

and safety of these sulfur-fumigated herbs (Wang et al., 2009). Recent studies have found that low sulfur dioxide residues do not affect the safety and efficacy of sulfurized herbs (Zhou et al., 2019). Nonetheless, many studies have shown that sulfur fumigation can cause chemical changes (He et al., 2018) affecting bioactivity (Yuan et al., 2019), respiratory system disorders (Wigenstam, Elfsmark, Bucht, & Jonasson, 2016), weakening immunomodulation (Ma et al., 2017), and even toxic effects on the liver and kidney (Jiang et al., 2020) in the long term. To date, there has been no report about the established analytical method for determining whether commercial MSCP samples undergo sulfur fumigation and whether sulfur fumigation alters the chemical composition of MSCP. Therefore, it is essential to explore a rapid, sensitive, reliable and confirmatory analytical-specific method to detect potential chemical changes and assess the quality of sulfur-fumigation MSCP.

Traditional phytochemical approaches have been used to isolate and identify individual components in herbs, but they are very difficult, time-consuming, costly and easily miss some potential small amounts of compounds (Li et al., 2012). HPLC-UV has often been applied to evaluate the quality of traditional Chinese medicine based on some known compounds, but it is difficult to apply this method to evaluate the unknown structures of new sulfur compounds (Zhang et al., 2021). These methods did not identify potential characteristic components to differentiate between the nonfumigation MSCP (NF-MSCP) and sulfur-fumigation MSCP (SF-MSCP) samples. Ultrahigh-performance liquid chromatography-quadrupole/time-of-flight mass spectrometry (UHPLC-QTOF-MS/MS), a powerful, rapid, and sensitive analytical approach, is extensively applied to isolate and identify the complex components in medicinal herbs (Chen et al., 2018; Ma et al., 2020; Zhang et al., 2022). Additionally, multivariate statistical analysis, such as unsupervised principal component analysis (PCA) and supervised orthogonal partial least-squares discriminate analysis (OPLS-DA), was used to analyze the holistic discrepancy and discover the potential chemical markers that contribute to differentiating between the NF-MSCP and SF-MSCP samples. Thus, it may be an ideal method for evaluating MSCP samples.

The purpose of this research was to explore a novel approach by using UHPLC-QTOF-MS/MS and multivariate statistical analysis to identify the chemical components of both NF-MSCP and SF-MSCP samples. Furthermore, the established approach was applied to discover the potential characteristic markers that could rapidly differentiate between NF-MSCP and SF-MSCP samples and gain insights into the potential structural transformation mechanism.

2. Materials and methods

2.1. Chemical reagents and materials

Acetonitrile and methanol were LC-MS grade and purchased from Fisher Scientific Co. (Loughb Orough, UK). Ultra-pure water was produced by a Milli-Q water purification system (Millipore, Bedford, USA). Other chemicals were of analytical grade.

Four reference compounds including hypaphorine, isoliquiritigenin, formononetin and maackiain, were purchased from the National

Institutes for Food and Drug Control (Beijing, China). The purity of the chemicals was determined to be more than 98 % by HPLC.

Ten batches of MSCP were obtained from different habitats of Guangxi Province. Commercial MSCP samples were obtained from different herbal markets in Yulin, Chengdu, Bozhou, Qinzhou and Nanning. The origins of all the samples were authenticated by Professor Zhifeng Zhang from the Institute of Qinghai-Tibetan Plateau, Southwest Minzu University, P. R. China, Sichuan, Chengdu. The details in this paper are shown in Table 1, and the samples were deposited in the medicine specimen room of Qin Zhou Provincial Health School (Qinzhou, China).

2.2. Instrumentation and chromatographic analytical conditions

The solutions were analyzed by a Waters ACQUITY UHPLC TM system (Waters Corporation, Milford, MA, USA) equipped with a binary solvent delivery manager, autosampler and PDA detector. The separation was conducted by an ACQUITY HSS T3 column (100 mm × 2.1 mm, 1.8 μm; Waters, USA) at 35 °C, and a 1 μL aliquot of extracting solution was injected into the UHPLC at a flow rate of 0.4 mL/min. A mobile phase composed of 0.1 % aqueous formic acid (A) and acetonitrile (B) was applied as follows: 5–8 % B (0–1.5 min), 8–12 % B (1.5–3 min), 12–30 % B (3–4.5 min), 30–35 % B (4.5–10 min), 35–40 % B (10–12 min), 40–65 % B (12–15 min), 65–85 % B (15–18 min), 85–95 % B (18–21 min), 95–5 % B (21–21.1 min), and 5–5 % B (21.1–25 min).

Mass spectrometry was performed using a Waters definition accurate mass quadrupole time-of-flight (Q-TOF) Xevo G2-S mass spectrometer (Waters MS Technologies, Manchester, UK). The scan range was set as 100–1500 Da. The capillary voltage of the positive and negative modes was set at 2.8 kV. The source and desolvation temperatures were set at 100 and 400 °C, respectively. The cone and desolvation gas flow rates were set at 20 and 800 L/h, respectively. The collision-induced dissociation (CID) was set at 6 V for the precursor ion and 35–50 V for fragmentation information. The reference was leucine-enkephalin ($[M-H]^- = 554.2615$ and $[M+H]^+ = 556.2771$), which could accurately measure the molecular masses from the precursor ions and product ions. Finally, the data were processed and analyzed using MassLynx 4.1 software (Waters Co., Milford, CT, USA).

2.3. Preparation of samples

Ten batches of MSCP samples were obtained from Qinzhou, Nanning and Shangxi of Guangxi Province in China. Fresh MSCP samples were washed and cut into thin slices (1 cm) for each batch. Then, half of the fresh MSCP samples were dried in sunlight, and the other half was dried by sulfur fumigation in a desiccator. Sulfur-fumigation procedures were carried out in accordance with farmers. First, fresh MSCP slices were placed in the upper layer in the desiccator. Second, the sulfur powder was put and burned in the bottom layer. When the whole desiccator was full of SO₂, the desiccator was then kept closed for 12 h. After fumigation, the MSCP slices were dried for 12 h at 40 °C.

2.4. Preparation of reference solutions

Reference stock solutions: Certain amounts of hypaphorine, isoliquiritigenin, formononetin and maackiain were dissolved in methanol/water (50 % v/v) to obtain four reference compound stock solutions, and each concentration was approximately equal to 1 mg/mL. A 0.1 mg/mL reference substance mixture solution was prepared by mixing and diluting the above four reference stock solutions. The reference substance mixture solution was further diluted and kept at 4 °C until further UHPLC-QTOF-MS/MS analysis.

2.5. Sample solution preparation

The dried sample was ground into powder, and 0.3 g of sample

powder with 10 mL of methanol/water (50 % v/v) solution was added into a 50 mL volumetric flask, and ultrasonic extraction was performed (Kun Shan Ultrasonic Instruments Co., Ltd., Kun Shan, China) at 40 kHz for 30 min at 35 °C. Then, the solution was filtered through a 0.22 μm millipore filter and analyzed by UHPLC-QTOF-MS/MS.

2.6. Data acquisition and analysis

Data acquisition was performed on a MassLynx 4.1 (Waters Corp., Milford, MA, USA). MarkerLynx XS software (Waters Corp., Milford, MA, USA) was used for processing and analysis of the data. The parameters were set as follows: initial retention time was set at 1 min, final retention time was set at 20 min, mass range was set at 100 to 1500 Da, mass tolerance was set at 0.01 Da, the mass window was set at 0.02 Da, and the retention time window was set at 0.02 min. Structural elucidation was analyzed with the Mass Fragment tool provided by MassLynx 4.1.

2.7. Determination of sulfur residues in MSCP samples

The sulfur residue content of MSCP was measured according to the Chinese Pharmacopoeia 2020 Edition (Volume IV) (Chinese Pharmacopoeia Commission, 2020). Ten grams of sample powder with 400 mL of distilled water and 10 mL of 6 mol/L HCl were added and distilled for 1.5 h in a sulfur dioxide assay apparatus, with flowing 0.2 L/min nitrogen. Then, 50 mL of 3 % hydrogen peroxide was mixed with 3 drops of 2.5 mg/mL methyl red ethanol indicator titrated by 0.01 mol/L NaOH to yellow in the conical flask, which was used to absorb the distillate. When the absorption liquid cooled to room temperature, it was titrated by 0.01 mol/L NaOH to yellow. Distilled water was used as the solvent for blank test correction. The result was calculated as shown in Eq. (1):

$$X = \frac{(V - V_0) \times 0.032 \times C \times 1000}{m} \quad (1)$$

X is the total sulfur dioxide in the samples (in SO₂), g/kg; V is the volume of NaOH standard solution used in the samples, mL; V₀ is the volume of NaOH standard solution used in the blank, mL; 0.032 represents 1 mL of NaOH standard solution (C = 1.0 mol/L) equivalent to the mass of sulfur dioxide, g; C is the concentration of NaOH standard solution, mol/L; and m is the sample mass, g.

2.8. Statistical analysis

To distinguish between NF-MSCP and SF-MSCP samples, the mass spectrum information was imported into SIMCA-P14.1 software for multivariate statistical analysis, including PCA and OPLS-DA. The S-plot from OPLS-DA together with the importance in the projection (VIP) were employed to select the potentially characteristic compounds. Information on fragment ions, reported literature and the established database was used to confirm the molecular formula and identify the compound. The cleavage process of the compound was conducted by the MS data of precursor ions and product ions.

3. Results and discussion

3.1. Optimization of chromatography and MS conditions

At present, there are no reports about the separation of sulfur compounds from MSCP. Therefore, it is necessary to develop a new detection approach to isolate and identify sulfur compounds because commercial MSCP may be sulfur-fumigated. In our previous study (Zhang et al., 2022), an ACQUITY HSS T3 column (100 mm × 2.1 mm, 1.8 μm) was employed to isolate and analyze NF-MSCP due to its better peak patterns and stronger separation ability. Therefore, the HSS T3 column was chosen for analysis in this study.

To obtain the best sensitivity for separation, various kinds of mobile

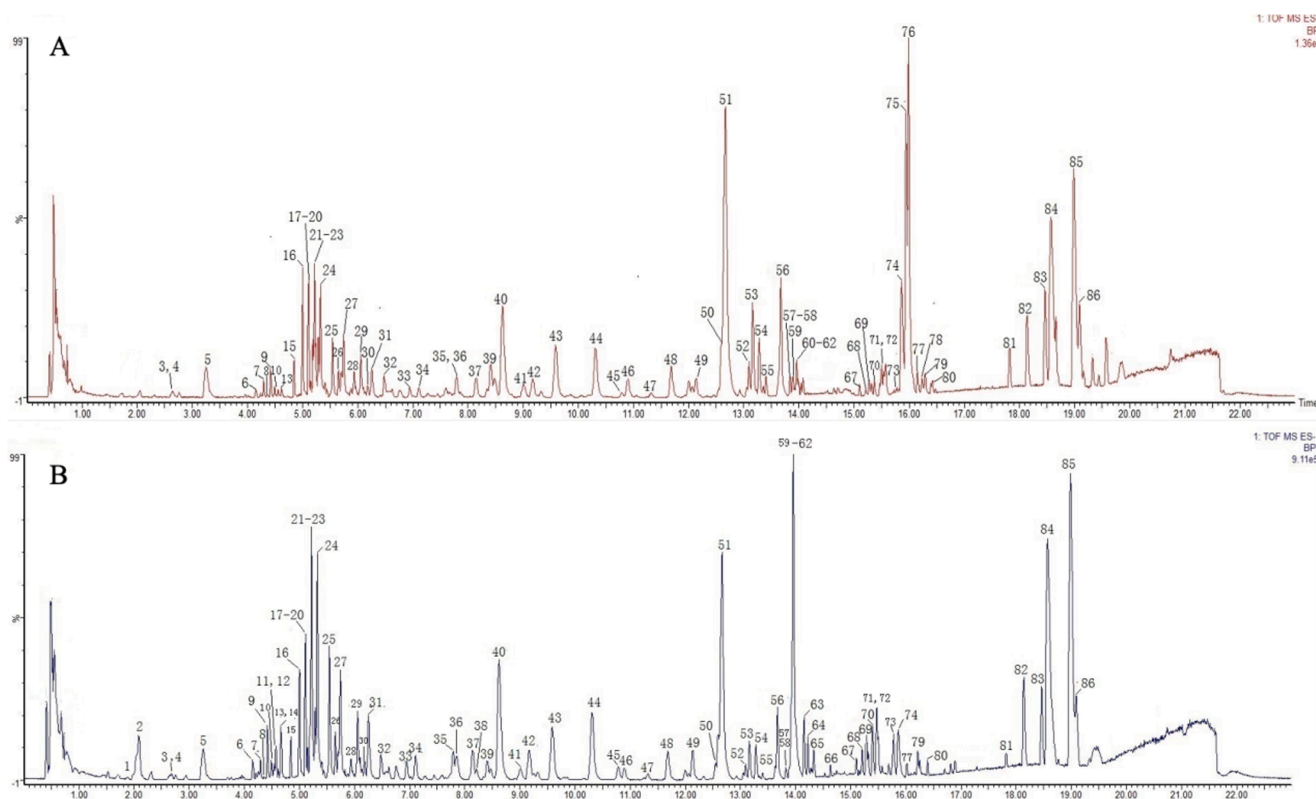


Fig. 1. Representative BPI chromatograms of MSCP samples. A: NF-MSCP; B: SF-MSCP;

phases were optimized, including acetonitrile–water, methanol–water, acetonitrile-0.1 % formic acid in water, methanol-0.1 % formic acid in water. The results indicated that the mixture of acetonitrile-0.1 % aqueous formic acid was appropriate for the mobile phase due to its better separation ability and more satisfactory peak patterns of the sample. The mass spectrometric parameters were also optimized, including collision energy, cone voltage, and capillary voltage. Under the optimized chromatographic and mass spectrometry conditions, a total of 86 peaks were separated and detected in the MSCP samples in negative mode within 20 min (Fig. 1).

3.2. Comparison of detectable components in NF-MSCP and SF-MSCP samples

In total, 86 chemical constituents were detected using our newly developed analytical method, 76 of which were detected in NF-MSCP and 83 in SF-MSCP. As shown in Fig. 1, most peak heights at retention times from 1 to 14 min increased after sulfur fumigation, and the peak heights of 16 major peaks (peaks 9, 10, 13, 21, 23, 23, 24, 25, 27, 31, 40, 49, 59, 60, 62 and 84) found in NF-MSCP sharply increased in SF-MSCP. However, most peak heights at retention times from 14 to 16 min displayed a declining trend, and the peak heights of 10 major peaks (peaks 39, 51, 52, 53, 54, 55, 56, 75, 76 and 78) detected in NF-MSCP showed a significant decline in SF-MSCP, and three of them (peaks 75, 76 and 78) even disappeared after sulfur fumigation. It was also found that 10 peaks (peaks 1, 2, 11, 12, 14, 38, 63, 64, 65 and 66) were newly generated as main peaks in SF-MSCP. These results indicated that sulfur fumigation induced the chemical transformation of the chemical constituents in MSCP. All the compounds identified in the NF-MSCP and SF-MSCP samples in the present work are shown in Table 2, including their retention time, molecular formula, and mass spectrometric information. Among them, 4 compounds were unambiguously confirmed by matching reference standards (peaks 5, 16, 41, and 69); however, the other compounds were tentatively identified by comparison with previously

reported MS data and literature information.

3.3. Identification of the chemical compounds of NF-MSCP

A total of 76 chemical constituents were detected in NF-MSCP, and 67 of them were identified or tentatively assigned, including 4 alkaloids, 6 flavanones, 51 terpenoids and 6 others. As shown in Table 2, compound 3 produced an $[M-H]^-$ ion at m/z 203.0821 with the molecular formula $C_{11}H_{12}N_2O_2$, and it further yielded fragment ions at m/z 142.0603 $[M-H-CH_2NO_2]^-$ and 116.0743 $[M-H-C_3H_6NO_2]^-$. Compound 3 was tentatively assigned as D-tryptophan. Compound 4 yielded an $[M-H]^-$ ion at m/z 216.0872. Compound 4 further produced fragment ions at m/z 198.0769, 2.0974, 115.0029, 100.0758, and 88.0394, and it was tentatively confirmed as L-callipeltose. Compound 5 displayed an $[M-H]^-$ ion at m/z 245.1290, and it further yielded fragment ions at m/z 186.0587 $[M-H-N(CH_3)_3]^-$ and 142.0677 $[M-H-N(CH_3)_3-CO_2]^-$. It was definitely identified as hypaphorine using the corresponding reference standard. Compound 9 showed an $[M+H]^+$ ion at m/z 263.1383, and it further generated fragment ions at m/z 204.1025, 176.0602, and 158.0597, and it was tentatively assigned as physovenine (Zhang, Cui, Lin, & Cai, 2021).

A total of 6 flavanones were tentatively assigned in NF-MSCP samples in this study. Compound 16 generated an $[M-H]^-$ ion at m/z 255.0663 with the formula $C_{15}H_{12}O_4$, which yielded fragment ions at 135.0124 and 119.0522. Compound 16 was unambiguously assigned as isoliquiritigenin by comparison with the corresponding reference standards. Similarly, compounds 41 and 69 were unambiguously confirmed as formononetin and maackiain, respectively, compared with the corresponding standard substances. Compounds 17 and 39 exhibited an $[M-H]^-$ ion at m/z 283.06 with the same formula $C_{16}H_{12}O_5$. Compound 17 further generated fragment ions at m/z 268.0379 and 151.0072, and it was tentatively confirmed as prunetin (Wang et al., 2021). Compound 39 further produced fragment ions at m/z 268.0356 and 135.0073, and it was tentatively identified as 5,4-dihydroxy-3'-methoxyisoflavone

Table 2

The results of UHPLC-QTOF-MS/MS identification of chemical constituents from NF-MSCP and SF-MSCP.

NO.	Retention time(min)	ESI-MS (m/z)	Error (ppm)	MS/MS fragments ions	Formula	Identification
1	1.97	283.0369 [M-H] ⁻	0.2	203.0821,142.0654,116.0502	C ₁₁ H ₁₂ N ₂ O ₅ S	D-Tryptophan sulfate
2	2.09	325.0844 [M-H] ⁻	0.5	266.0110,222.0215,142.0647,116.0489	C ₁₄ H ₁₈ N ₂ O ₅ S	Hypaphorine sulfate
3	2.63	203.0821 [M-H] ⁻	1.2	142.0603,116.0743	C ₁₁ H ₁₂ N ₂ O ₂	D-Tryptophan
4	2.67	216.0872 [M-H] ⁻	2.1	198.0769,172.0974,115.0029,100.0758,88.0394	C ₉ H ₁₅ NO ₅	L-Callipeltose
5	3.26	245.1290 [M-H] ⁻	1.3	187.0609,186.0587,142.0677	C ₁₄ H ₁₈ N ₂ O ₂	Hypaphorine
6	4.15	581.1509 [M-H] ⁻	0.5	567.1358,419.1727,259.0613,241.0719	C ₂₆ H ₃₀ O ₁₅	Polygalaxanthone V
7	4.29	611.1612 [M-H] ⁻	0.9	341.0912,299.0587	C ₂₇ H ₃₂ O ₁₆	Unknown
8	4.35	505.1713 [M-H] ⁻	1.1	490.1404,475.1198,340.0756,328.0742	C ₂₅ H ₃₀ O ₁₁	Shomaside E
9	4.42	263.1383 [M + H] ⁺	1.2	ESI ⁺ 204.1025,176.0602,158.0597	C ₁₄ H ₁₈ N ₂ O ₃	physovenine
10	4.49	583.1660 [M-H] ⁻	-0.5	433.1331,301.0923,167.0343,152.0107,123.0443,108.0207	C ₂₆ H ₃₂ O ₁₅	seguinoid K
11	4.54	335.0279 [M-H] ⁻	-3.0	255.0653,135.0079,119.0509	C ₁₅ H ₁₂ O ₇ S	Isoliquiritigenin sulfate
12	4.58	363.0221 [M-H] ⁻	1.4	283.0600,269.0432,255.0662,167.0330	C ₁₆ H ₁₂ O ₈ S	Prunetin sulfate
13	4.62	453.3446 [M + H] ⁺	2.0	ESI ⁺ 435.3313,407.3292,313.2197,285.1837,	C ₃₀ H ₄₄ O ₃	Unknown
14	4.68	351.0168 [M-H] ⁻	-2.8	230.9562,120.0801	C ₁₅ H ₁₂ O ₈ S	Naringenin sulfate
15	4.84	564.4132 [M-H] ⁺	3.1	546.4023,337.2608,281.2479,241.1866,225.2604	C ₂₉ H ₅₉ NO ₉	Unknown
16	5.00	255.0663 [M-H] ⁻	2.4	135.0124,119.0522	C ₁₅ H ₁₂ O ₄	Isoliquiritigenin
17	5.06	283.0606 [M-H] ⁻	1.5	268.0379,254.1822,151.0072,118.0420	C ₁₆ H ₁₂ O ₅	Prunetin
18	5.11	790.5717 [M-H] ⁻	0.8	772.5717,451.3281,338.2433,225.1587,193.0880	C ₄₆ H ₈₁ NO ₉	Unknown
19	5.15	1089.5530 [M-H] ⁻	4.4	939.4581,909.3250,793.4388,778.2282,442.2473	C ₅₃ H ₈₆ O ₂₃	Soyasapogrol B 3-O-α-L-arabinopyranosyl-(1 → 2)-β-D-galactopyranosyl-(1 → 2)-glucuronopyranosyl-22-O-β-D-glucopyranoside
20	5.19	1119.5635 [M-H] ⁻	4.3	939.4543,793.4285	C ₅₄ H ₈₈ O ₂₄	3β,22,24-trihydroxyolean-12-en-29-oic acid 3-O-α-L-rhamnopyranosyl-(1 → 2)-β-D-galactopyranosyl-(1 → 2)-glucopyranosyl-22-O-β-D-glucopyranoside
21	5.22	1119.5634 [M-H] ⁻	4.3	1101.5586,973.4937,911.5079,793.4413,749.4536,587.3992,205.0721,163.0608,	C ₅₄ H ₈₈ O ₂₄	23-hydroxyl pomalic acid 3-o-α-l-rhamnopyranosyl- (1 → 4)-β-d-glucopyranosyl-(1 → 6)-β-d-galactopyranosyl-28-o-β-d-glucopyranoside

(continued on next page)

Table 2 (continued)

NO.	Retention time(min)	ESI-MS (m/z)	Error (ppm)	MS/MS fragments ions	Formula	Identification
22	5.24	1087.5355 [M-H] ⁻	2.8	941.4936,879.4833,473.3639,205.0746,179.0568,163.0615	C ₅₃ H ₈₄ O ₂₃	Oleanolic acid 3-O- α -L-rhamnopyranosyl-(1 \rightarrow 2)- β -D-glucopyranosyl-(1 \rightarrow 2)- β -D-galactopyranosyl-28-O- β -D-glucopyranoside
23	5.29	1117.5487 [M-H] ⁻	4.5	1099.5398,1055.5522,971.4926,953.4879,927.4984,909.5012,791.4277,773.4124,633.4033,205.0717,163.0604	C ₅₄ H ₈₆ O ₂₄	3 β ,22,24-trihydroxyolean-12-en-29-oic acid 3-O- α -L-rhamnopyranosyl-(1 \rightarrow 2)- α -L-rhamnopyranosyl-(1 \rightarrow 2)- β -D-glucuronopyranoyl-22-O- β -D-glucopyranoside
24	5.32	1117.5476 [M-H] ⁻	4.0	971.4926,955.4874,909.5012,791.4277,485.3267,205.0717	C ₅₄ H ₈₆ O ₂₄	3 β -olean-12-en-28,29-dioic acid 3-O- α -L-rhamnopyranosyl-(1 \rightarrow 2)- β -D-glucopyranosyl-(1 \rightarrow 2)- β -D-galactopyranosyl-28-O- β -D-glucopyranoside
25	5.54	1103.5685 [M-H] ⁻	4.3	1085.5488,957.5008,941.4578,777.4440,485.3300,403.1258,205.0720	C ₅₄ H ₈₈ O ₂₃	Soyasapogrol B 3-O- α -L-rhamnopyranosyl-(1 \rightarrow 2)- β -D-galactopyranosyl-(1 \rightarrow 2)-glucuronopyranosyl-22-O- β -D-glucopyranoside
26	5.65	1071.5372 [M-H] ⁻	2.2	939.4546,909.3124,867.4311,775.3973,764.4250,617.1602,455.3395	C ₅₃ H ₈₄ O ₂₂	Betulinic acid 3-O- α -L-arabinopyranosyl-(1 \rightarrow 2)- α -L-rhamnopyranosyl-(1 \rightarrow 2)- β -D-glucuronopyranosyl-28-O- β -D-glucopyranoside
27	5.74	1101.5529 [M-H] ⁻	4.3	955.4899,893.4901,775.4259,757.4174,205.0713,179.0555,163.0602,143.0347	C ₅₄ H ₈₆ O ₂₃	Oleanolic acid 3-O- α -L-rhamnopyranosyl-(1 \rightarrow 2)- β -D-galactopyranosyl-(1 \rightarrow 2)-glucuronopyranosyl-28-O- β -D-glucopyranoside
28	5.93	1101.5524 [M-H] ⁻	3.8	955.4751,939.4596,793.3958,599.3540,455.1577	C ₅₄ H ₈₆ O ₂₃	Betulinic acid 3-O- α -L-rhamnopyranosyl-(1 \rightarrow 2)- β -D-galactopyranosyl-(1 \rightarrow 2)-glucuronopyranosyl-28-O- β -D-glucopyranoside
29	6.06	1131.5275 [M-H] ⁻	4.6	1087.5253,985.4680,823.4686,205.0687,179.0540,163.0590	C ₅₄ H ₈₄ O ₂₅	3 β -olean-12-en-28,29-dioic acid 3-O- α -L-rhamnopyranosyl-(1 \rightarrow 2)- β -D-galactopyranosyl-(1 \rightarrow 2)-glucuronopyranosyl-28-O- β -D-glucopyranoside
30	6.19	1073.5573 [M + HCOO] ⁻	2.8	455.1127,429.1175	C ₅₂ H ₈₄ O ₂₀	Oleanolic acid 3-O- α -L-arabinopyranosyl-(1 \rightarrow 2)- α -L-rhamnopyranosyl-(1 \rightarrow 2)-[α -L-arabinopyranosyl-(1 \rightarrow 3)]- β -D-galactopyranoside
31	6.25	969.4728 [M-H] ⁻	3.4	951.4692,907.4745,823.4053,779.4261,761.4124,743.4004,643.3489,617.3655,599.3583,485.3264,467.3167,205.0695,163.0600	C ₄₈ H ₇₄ O ₂₀	milletiasaponin B

(continued on next page)

Table 2 (continued)

NO.	Retention time(min)	ESI-MS (m/z)	Error (ppm)	MS/MS fragments ions	Formula	Identification
32	6.48	1071.5410 [M-H] ⁻	3.2	939.4578,909.3109,863.4765,793.3577,775.4262,617.1602,205.0711,179.0543,163.0592	C ₅₃ H ₈₄ O ₂₂	Oleanolic acid 3-O-α-L-arabinopyranosyl-(1 → 2)-α-L-rhamnopyranosyl-(1 → 2)-β-D-glucuronopyranosyl-28-O-β-D-glucopyranoside
33	6.94	1115.5316 [M-H] ⁻	3.8	969.4653,955.4852,807.4099,630.3679,545.2197,205.0694	C ₅₄ H ₈₄ O ₂₄	28-GlucosyloleanolicAcid3-[Rhamnosyl-(1 → 2)-Galactosyl-(1 → 3)-Glucuronide]
34	7.11	953.4763 [M-H] ⁻	1.8	925.4781,807.4175,645.1835,469.3312,205.0694,163.0599	C ₄₈ H ₇₄ O ₁₉	3α-hydroxy-11-oxoolean-12-en-30-oic acid 3-O-α-L-rhamnopyranosyl-(1 → 2)-β-D-galactopyranosyl-(1 → 2)-glucuronopyranoside
35	7.79	969.4703	0.8	951.4592,823.4108,779.4122,761.4146,643.3506,601.3727, 485.3394,205.0721,163.0616	C ₄₈ H ₇₄ O ₂₀	Abrisaponin I
36	7.84	955.4916 [M-H] ⁻	1.4	937.4827,809.4239,630.3730,471.3493,205.0711,163.0611	C ₄₈ H ₇₆ O ₁₉	Saponin A
37	8.15	983.4875 [M-H] ⁻	2.3	965.4771,939.4827,921.4828,879.4709,837.4296,751.4257,733.4155,687.3705,645.3610,529.3487,487.3406,469.3267,205.0711,163.0608	C ₄₉ H ₇₆ O ₂₀	Wistaria-Saponin G
38	8.21	875.4055 [M-H] ⁻	-5.3	795.4521,537.3282,457.3607	C ₄₂ H ₆₈ O ₁₇ S	Soyasaponin III sulfate
39	8.4	283.0613 [M-H] ⁻	0.4	268.0356,135.0073,	C ₁₆ H ₁₂ O ₅	5,4'-dihydroxy-3'-methoxyiso-flavone
40	8.62	1013.4966 [M-H] ⁻	0.9	909.4848,806.4464,763.4246,645.3632,601.3739,529.3506,487.3423,469.3312	C ₅₀ H ₇₈ O ₂₁	milletiasaponin A
41	9.00	267.0657 [M-H] ⁻	0.2	252.0425,223.0397,208.0503,195.0453,135.0103,132.0213	C ₁₆ H ₁₂ O ₄	Formononetin
42	9.16	791.4187 [M-H] ⁻	0.7	733.4240,645.3698,601.3768,441.3310,439.3253	C ₄₂ H ₆₄ O ₁₄	3α-hydroxy-11-oxoolean-12-en-30-oic acid 3-O-α-L-rhamnopyranosyl-(1 → 2)-β-D-glucuronopyranoside
43	9.58	867.4397 [M-H] ⁻	2.2	705.3782,703.3315,687.3762,529.3535	C ₄₄ H ₆₈ O ₁₇	1β-[(2-O-α-L-rhamnopyranosyl-α-L-arabinopyranosyl)oxy]-26-(β-D-glucopyranosyloxy) furosta-5,20(22),25(27)-trien-3β-ol
44	10.3	997.5063 [M-H] ⁻	5.5	979.4883,935.5049,893.4923,851.4468,833.4354,789.4446,671.3807,653.3724,471.3477,205.0717,163.0613	C ₅₀ H ₇₈ O ₂₀	22β-acetyloxy-3β,24-dihydroxyolean-12-en-29-oic acid 3-α-L-rhamnopyranosyl-(1 → 2)-β-D-galactopyranosyl-(1 → 2)-glucuronopyranoside
45	10.78	999.5193 [M-H] ⁻	2.8	853.4432,673.3847,529.2606,471.1714	C ₅₀ H ₈₀ O ₂₀	Asiaticoside C
46	10.9	997.5044 [M-H] ⁻	3.6	979.4898,935.5024,893.4882,851.4393,833.4354,765.4454,747.4323,729.4205,529.2516,471.3477	C ₅₀ H ₇₈ O ₂₀	Unknown
47	11.32	645.3649 [M-H] ⁻	1.5	483.3116,465.3030,421.3070,327.2296	C ₃₆ H ₅₄ O ₁₀	abrusoside A
48	11.68	851.4454 [M-H] ⁻	2.9	765.4376,747.4301,671.3658,629.3654,603.3936,471.3475	C ₄₄ H ₆₈ O ₁₆	3-((3'-Malonyl)Xyl)-28-Glu-2-Hydroxy Oleanolic Acid
49	12.13	967.4920 [M-H] ⁻	1.8	949.4747,923.4655,905.4879,821.4285,803.4280,759.4307,615.3815,581.3735,553.3500,471.3467,205.0717,163.0612	C ₄₉ H ₇₆ O ₁₉	Dumortierioside A Methyl Ester

(continued on next page)

Table 2 (continued)

NO.	Retention time(min)	ESI-MS (m/z)	Error (ppm)	MS/MS fragments ions	Formula	Identification
50	12.54	997.5014 [M-H] ⁻	0.4	979.4917,925.5134,807.4156,629.3702,618.2419,205.0717,163.0604	C ₅₀ H ₇₈ O ₂₀	Unknown
51	12.68	941.5134 [M-H] ⁻	2.5	923.4998,795.4317,615.3881,597.3771,457.3674,205.0714,163.0608	C ₄₈ H ₇₈ O ₁₈	Soyasaponin I
52	13.09	795.4553 [M-H] ⁻	2.8	633.3791,615.3702,457.2651	C ₄₂ H ₆₈ O ₁₄	Soyasaponin III
53	13.16	911.5041 [M-H] ⁻	4.1	893.4884,765.4325,615.3879,457.3669,205.0710,163.0603,	C ₄₇ H ₇₆ O ₁₇	Soyasaponin II
54	13.28	925.5197 [M-H] ⁻	3.9	907.5051, 599.3842,509.4007, 457.3653	C ₄₈ H ₇₈ O ₁₇	Soyasapogrnol B 3-O-α-L-arabinopyranosyl-(1 → 2)-α-L-rhamnopyranosyl-(1 → 2)-β-D-glucuronopyranoside
55	13.4	925.5185 [M-H] ⁻	2.6	907.5051,779.4551,763.4258,599.3937,441.3755	C ₄₈ H ₇₈ O ₁₇	Kaikasaponin III
56	13.67	939.4980 [M-H] ⁻	2.9	793.4335,775.4265,631.3806,455.3508,205.0709,163.0601	C ₄₈ H ₇₆ O ₁₈	Oleanolic acid 3-O-α-L-rhamnopyranosyl-(1 → 2)-β-D-galactopyranosyl-(1 → 2)-glucuronopyranoside
57	13.84	895.5074 [M-H] ⁻	2.0	599.3906,509.3978,439.3560,205.0710,163.0602	C ₄₇ H ₇₆ O ₁₆	Oleanolic acid 3-O-α-L-arabinopyranosyl-(1 → 2)-α-L-rhamnopyranosyl-(1 → 2)-β-D-galactopyranoside
58	13.84	1065.5299 [M-H] ⁻	2.7	1047.5105,1033.4703,902.4802,740,3681	C ₅₄ H ₈₂ O ₂₁	unknown
59	13.89	895.5071 [M-H] ⁻	1.8	565.3868,509.4007,439.3576,205.0710,163.0601	C ₄₇ H ₇₆ O ₁₆	Betulinic acid 3-O-α-L-arabinopyranosyl-(1 → 2)-α-L-rhamnopyranosyl-(1 → 2)-β-D-galactopyranoside
60	13.91	1037.5364 [M-H] ⁻	4.1	1019.5126,741.4143,583.3978,247.0903,205.0714,163.0589,157.0128,143.0354,131.0342,125.0236,113.0245	C ₅₃ H ₈₂ O ₂₀	Soyasaponin Betaa
61	13.91	1067.5472 [M-H] ⁻	4.2	1049.5487,921.4904,741.4242,583.3993,457.3721	C ₅₄ H ₈₄ O ₂₁	Soyasaponin VI
62	13.96	763.4257 [M-H] ⁻	0.8	617.4031,437.3429	C ₄₁ H ₆₄ O ₁₃	Oleanolic acid 3-O-α-L-rhamnopyranosyl-(1 → 2)-β-D-galactopyranoside
63	14.16	793.4381 [M-H] ⁻	-1.6	631.3919,437.3062,163.0617	C ₄₂ H ₆₆ O ₁₄	Ginsenoside Z-R1
64	14.22	921.4867 [M-H] ⁻	1.8	777.4570,759.4265,597.3782, 437.3411, 163.0612,	C ₄₈ H ₇₄ O ₁₇	Soyasaponin Gammag
65	14.33	759.4333 [M-H] ⁻	1.2		C ₄₂ H ₆₄ O ₁₂	3-Glucuronyl-22-DDMP
66	14.63	537.3287 [M-H] ⁻	6.9	457.3633	C ₃₀ H ₅₀ O ₆ S	Soyasapogenol B Soyasapogenol B sulfate
67	15.15	271.0603 [M-H] ⁻	0.9	151.0073,119.0472	C ₁₅ H ₁₂ O ₅	Naringenin
68	15.21	471.3461 [M + HCOO] ⁻	2.3	410.1615	C ₂₉ H ₄₆ O ₂	7-oxostigmasterol
69	15.28	283.0614 [M-H] ⁻	0.3	268.0379,239.0349	C ₁₆ H ₁₂ O ₅	Maackiain
70	15.4	313.2390 ([M-H] ⁻	3.5	-	C ₁₈ H ₃₃ O ₄	Octadecanedioic acid

(continued on next page)

Table 2 (continued)

NO.	Retention time(min)	ESI-MS (m/z)	Error (ppm)	MS/MS fragments ions	Formula	Identification
71	15.47	409.2383 [M-H] ⁻	1.0	391.2249,260.8799,241.0142	C ₂₆ H ₃₄ O ₄	Unknown
72	15.5	633.3798 [M-H] ⁻	1.1	589.3909,453.3358,179.0345,163.0409,135.0444	C ₃₉ H ₅₄ O ₇	Myriceric acid B
73	15.77	295.2298 [M-H] ⁻	7.5	277.2181	C ₁₈ H ₃₂ O ₃	9-hydroxy-10,12-octadecadienoic acid
74	15.86	540.3309 [M + HCOO] ⁻	4.3	255.2315,224.0683,168.0460	C ₂₇ H ₄₇ N ₃ O ₈	unknown
75	15.94	617.3841 [M-H] ⁻	-3.1	573.3528,437.3425,179.0337,163.0414,134.0366	C ₃₉ H ₅₄ O ₆	Pyracrenic acid
76	15.99	617.3847 [M-H] ⁻	0.8	573.3528,437.3414,163.0146,145.02896	C ₃₉ H ₅₄ O ₆	3-O-Caffeoyloleanolic acid
77	16.09	633.3792 [M-H] ⁻	0.8	589.3902,473.2837,179.0361,163.0410,135.0459	C ₃₉ H ₅₄ O ₇	2-O-Caffeoyl Maslinic Acid
78	16.16	633.3798 [M-H] ⁻	1.1	589.3906,453.3407,179.0342,163.0402,135.0447	C ₃₉ H ₅₄ O ₇	2α-Hydroxypyracrenic acid
79	16.25	647.3947 [M-H] ⁻	-0.2	633.3776,615.3176,409.2353,179.0344,161.0225	C ₄₀ H ₅₆ O ₇	Eucalyptolic acid
80	16.39	795.4116 [M-H] ⁻	1.0	633.3787,615.3682,571.3779,543.3683,179.0346,161.0236,135.0438	C ₄₈ H ₆₀ O ₁₀	Myriceric acid C
81	17.82	617.3851 [M-H] ⁻	1.5	471.3428,453.3366,147.0441	C ₃₉ H ₅₄ O ₆	Isoneriucoumaric acid
82	18.14	617.3856 [M-H] ⁻	2.3	471.3388,453.3426,146.9675	C ₃₉ H ₅₄ O ₆	27-p-Coumaroyloxyursolic acid
83	18.46	455.3527 [M-H] ⁻	0.4	439.3582	C ₃₀ H ₄₈ O ₃	Betulinic acid
84	18.57	455.3522 [M-H] ⁻	-0.7	439.3544,231.1741,173.1318	C ₃₀ H ₄₈ O ₃	Oleanolic acid
85	18.99	603.4058 [M-H] ⁻	1.5	179.0341,161.0240,134.0367	C ₃₉ H ₅₆ O ₅	Betulin-3-caffeate
86	19.09	603.405 [M-H] ⁻	0.3	179.0333,161.0240,134.0364	C ₃₉ H ₅₆ O ₅	Uvaol-3-caffeate

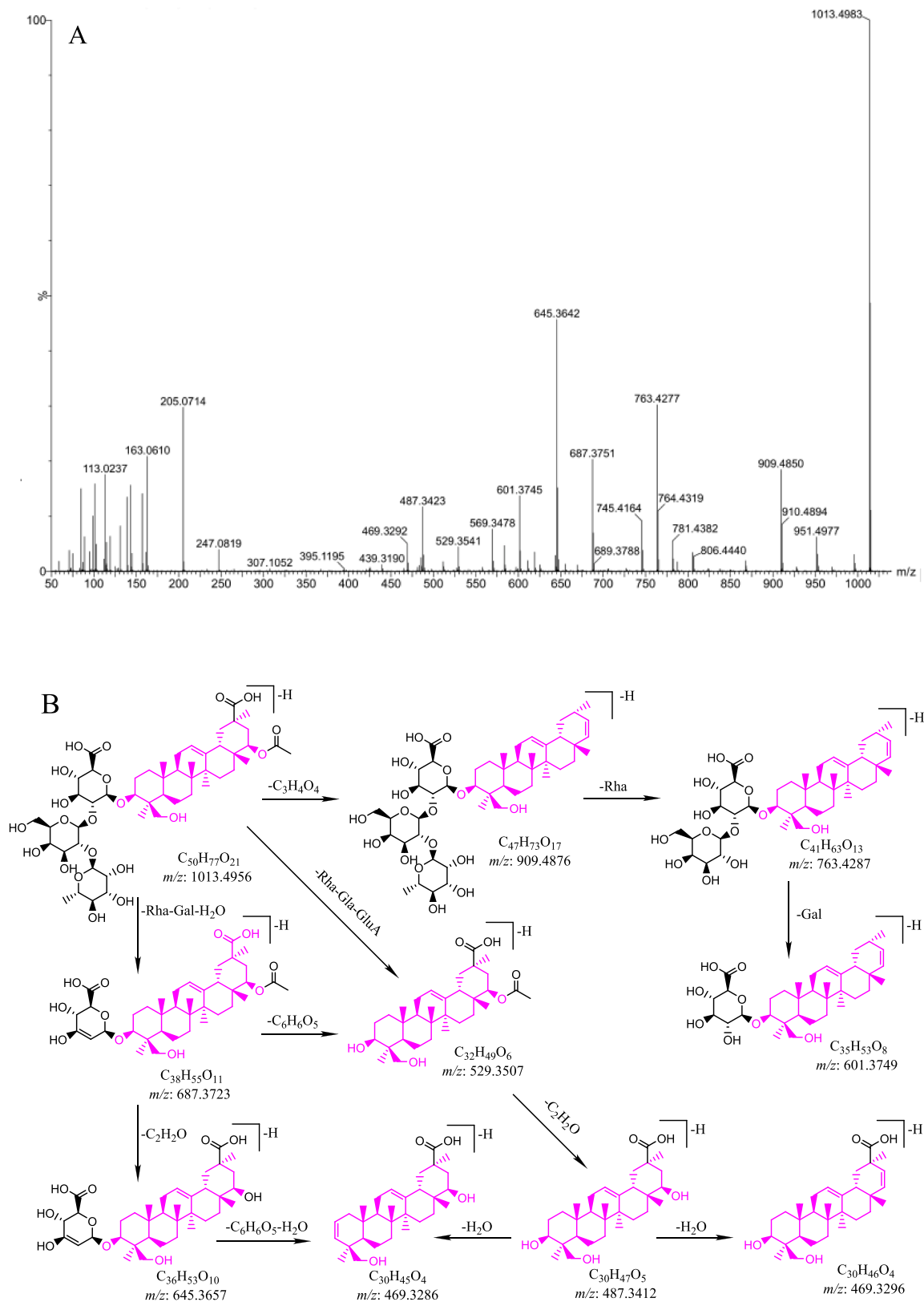


Fig. 2. A: The MS/MS spectrum in negative mode of compound 40; B: hypothesized fragmentation pathway of compound 40;

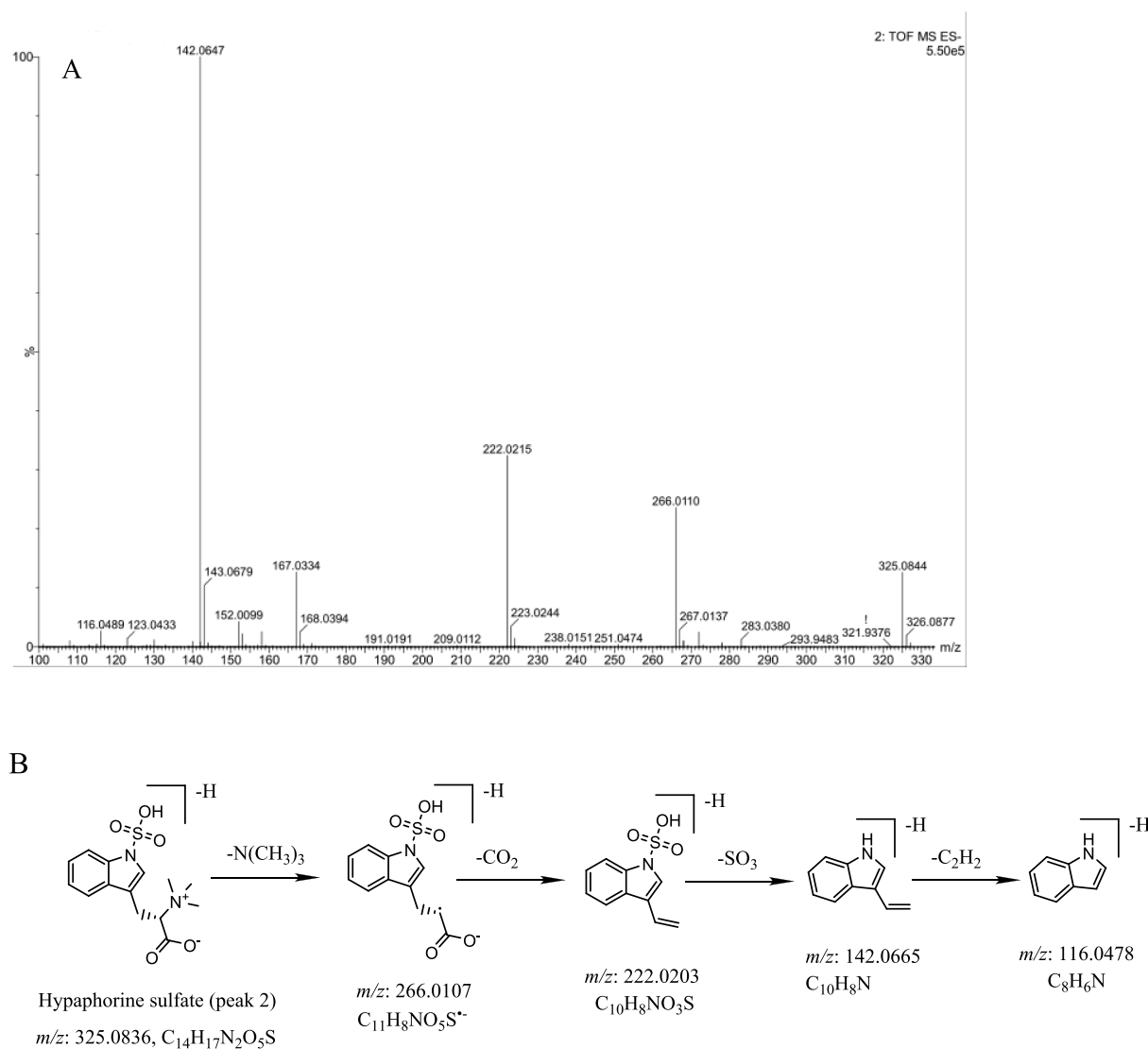


Fig. 3. A: The MS/MS spectrum in negative mode of compound 2; B: The hypothesized fragmentation pathway of compound 2;

(Wang et al., 2021). Compound 67 showed an $[M-H]^-$ ion at m/z 271.0603 with product ions at 151.0073 and 119.0472, and it was tentatively assigned as naringenin (Fu et al., 2016).

As shown in Table 2, 51 terpenoids were tentatively confirmed in NF-MSCP samples in this study. Compound 40 was used as a detailed example to demonstrate the fragmentation patterns of terpenoids. Compound 40 yielded an $[M-H]^-$ ion at m/z 1013.4966 with the formula $C_{50}H_{78}O_{21}$, which further yielded fragment ions at m/z 909.4848 $[M-H-C_3H_4O_4]^-$, 763.4246 $[M-H-C_3H_4O_4-Rha]^-$, 687.3744 $[M-H-Rha-Gal-H_2O]^-$, 645.3632 $[M-H-Rha-Gal-H_2O-C_2H_2O]^-$, 601.3739 $[M-H-C_3H_4O_4-Rha-Gal]^-$, 529.3506 $[M-H-Rha-Gal-GluA]^-$, 487.3423 $[M-H-Rha-Gal-GluA-C_2H_2O]^-$, and 469.3312 $[M-H-Rha-Gal-GluA-C_2H_2O-H_2O]^-$. Therefore, compound 40 was tentatively assigned as milletiasaponin A, according to a previous report in MSCP (Uchiyama et al., 2003). The mass spectra in negative mode and the hypothesized fragmentation pathway of compound 40 are shown in Fig. 2. By a similar pathway, compounds 19, 20, 21, 22, 23, 24, 25, 26, 27, 28, 29, 30, 31, 32, 33, 34, 42, 44, 47, 51, 52, 53, 54, 56, 57, 59 and 62 were identified as terpenoid glycosides according to the fragmentation and the Clog P values, which had been previously reported in the literature (Zhao et al., 2017; Wang et al., 2021; Zhang, Cui, Lin, & Cai, 2021). Compounds 35, 36, 37, 55, 60, 61, 83 and 84 have previously been reported in the same species (Chiang & Chang, 1982; Massiot,

Lavaud, Benkhaled, & Men-Olivier, 2004; Shi, Wen, & Tu, 2006; Ha et al., 2014) and have been identified in MSCP. In a similar manner, compounds 43, 45, 48, 49, 72, 75, 76, 77, 78, 79, 80, 81, 82, 85 and 86 were tentatively assigned as terpenoid glycosides by comparison with their fragment ions.

In this study, six constituents attributed to fatty acids and other compounds were identified. Compound 6 possessed an $[M-H]^-$ ion at m/z 581.1509, and it further generated fragment ions at m/z 567.1358 $[M-CH_3]^-$, 419.1727 $[M-H-CH_3-Rha]^-$, 259.0613 $[M-H-CH_3-Rha-Glu]^-$, and 241.0719 $[M-H-CH_3-Rha-Glu-H_2O]^-$. Therefore, it was tentatively identified as polygalaxanthone V by comparison with the related literature (Zhang, Cui, Lin, & Cai, 2021). According to the fragmentation ions and related literature, compounds 8, 10, 68, 70 and 73 were tentatively deduced as shomaside E, seguinoside K (Yin et al., 2008), 7-oxostigmasterol, octadecanedioic acid (Wang et al., 2021), and 9-hydroxy-10,12-octadecadienoic acid, respectively.

3.4. Elucidating the identification of sulfate compounds of SF-MSCP

Ten markers (peaks 1, 2, 11, 12, 14, 38, 63, 64, 65 and 66) were detected in the 70 % methanol extract of the SF-MSCP sample. Among them, compounds 63, 64 and 65 were regarded as terpenoid metabolites, and the other 7 compounds (peaks 1, 2, 11, 12, 14, 38 and 66) were

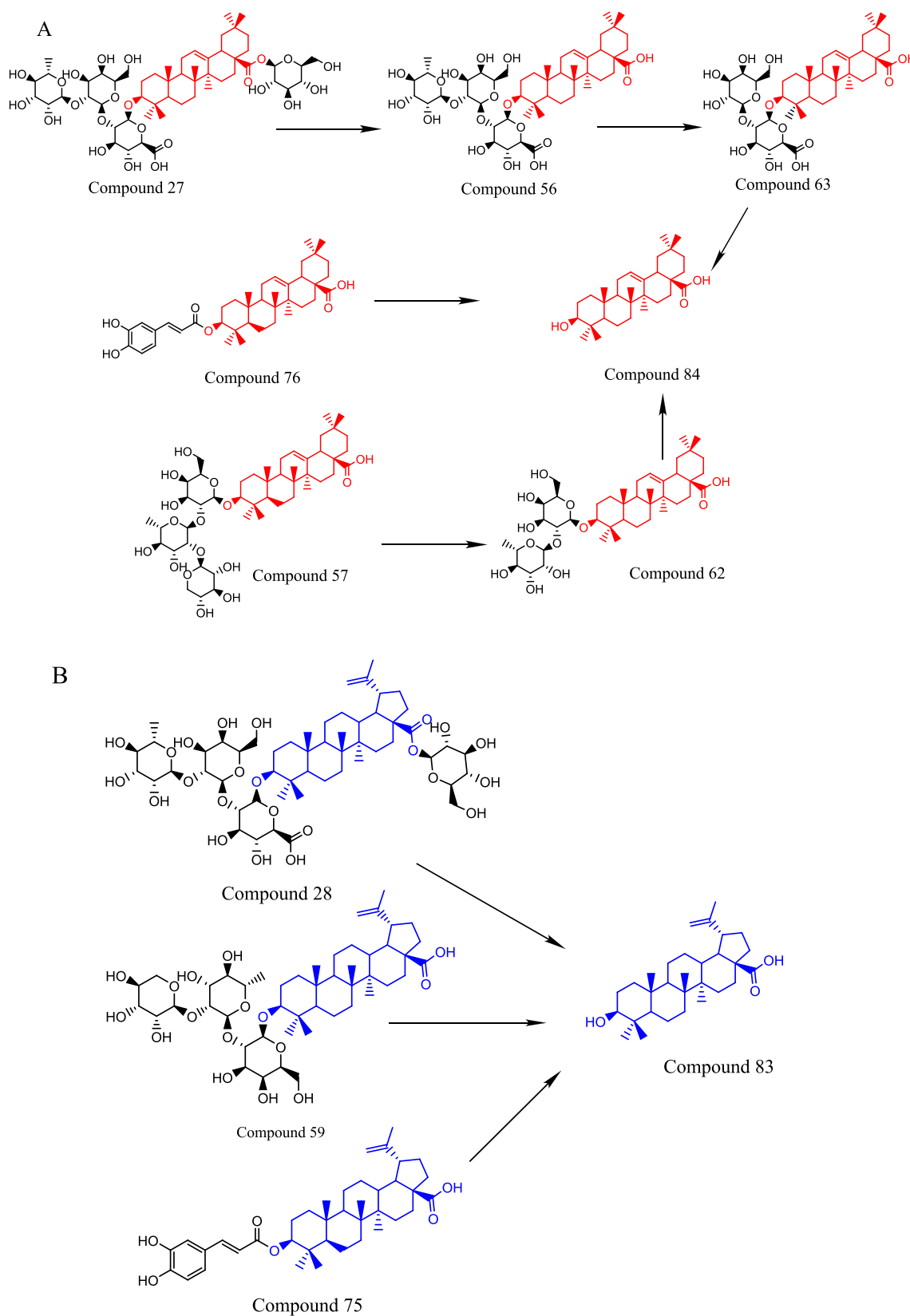


Fig. 4. A: Possible transformation mechanism of Oleanoic acid type; B: Possible transformation mechanism of Betulinic acid type; C: Possible transformation mechanism of Soyasapogenol B type.

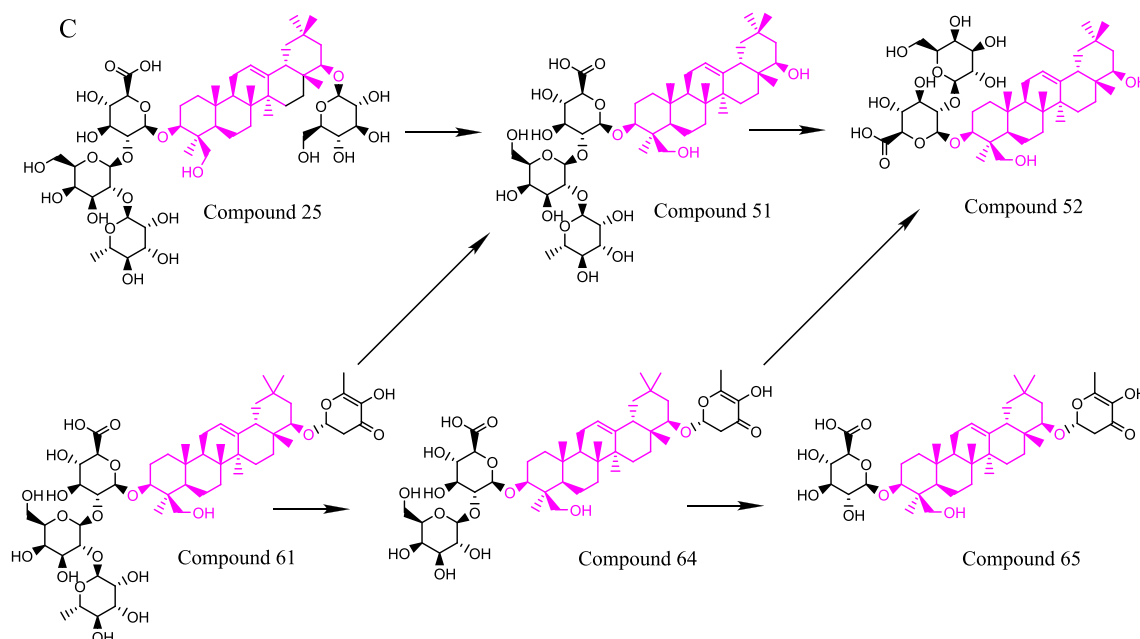


Fig. 4. (continued).

identified as sulfate derivatives according to the confirmed molecular and fragment ions. Compound 63 gave an $[M-H]^-$ ion at m/z 793.4381, and it further generated fragment ions at m/z 731.4019 $[M-H-Gal]^-$ and 437.3062 $[M-H-Gal-GluA]^-$. Thus, compound 63 was tentatively identified as zingibroside R1. In the same manner, compounds 64 and 65 were tentatively recognized as soyasaponin gammag and 3-glucuronyl-22-DDMP soyasapogenol B.

Seven sulfate derivatives were identified in the present SF-MSCP samples. Two alkaloid sulfate compounds (1 and 2) were tentatively identified. Compound 2 generated an $[M-H]^-$ ion at m/z 325.0858, 80 Da more than that of hypaphorine (5) ($C_{14}H_{18}N_2O_2$, m/z 245.1290). Its empirical molecular formula $C_{14}H_{18}N_2O_5S$ indicated an exact “ SO_3 ” addition to hypaphorine, and it further produced 266.0110, 222.0215, 142.0647 and 116.00489 corresponding to the successive loss of $N(CH_3)_3$, CO_2 and SO_3 . The mass spectra in negative mode and hypothesized fragmentation pathways of compound 2 are shown in Fig. 3A-B. Therefore, compound 2 was tentatively identified as hypaphorine sulfate. Similarly, compound 1 was tentatively assigned as D-tryptophan sulfate. It showed an $[M-H]^-$ ion at m/z 283.0369, 80 Da more than that of D-tryptophan (3) ($C_{11}H_{12}N_2O_2$, m/z 203.0821). Its empirical molecular formula $C_{11}H_{12}N_2O_5S$ suggested an exact “ SO_3 ” addition to D-tryptophan. The characteristic fragment ions at m/z 203.0821, 142.0654 and 116.0502 were regarded as successive losses of SO_3 , $HNCOOH$ and C_2H_2 , respectively.

Similarly, three flavanone sulfate compounds (11, 12 and 14) were tentatively identified. Compound 11 yielded an $[M-H]^-$ ion at m/z 335.0279 with the molecular formula $C_{15}H_{12}O_7S$, indicating an exact “ SO_3 ” addition to isoliquiritigenin (16) ($C_{15}H_{12}O_4$, m/z 255.0663), and it further generated 255.0653, 135.0079 and 119.0509. A fragment ion at m/z 255.0653 corresponded to the loss of SO_3 . Compound 11 was tentatively assigned as isoliquiritigenin sulfate. Compound 12 had an accurate mass at m/z 363.0221, 80 Da more than that of prunetin (17) ($C_{16}H_{12}O_5$, m/z 283.0606). Its empirical molecular formula $C_{16}H_{12}O_8S$ indicated an exact “ SO_3 ” addition to prunetin. Fragment ions at m/z 283.0600, 269.0432, 255.0662 and 167.0330 were observed, and compound 12 was tentatively deduced to be prunetin sulfate. Compound 14 showed an $[M-H]^-$ ion at m/z 351.0528 with the formula $C_{15}H_{12}O_8S$, which was 80 Da more than that of naringenin (67) ($C_{15}H_{12}O_5$, m/z 271.0603), showing an exact “ SO_3 ” addition to naringenin. Compound 14 also displayed an $[M+H]^+$ ion at 353.0378 in positive ion mode. The

fragment ions at m/z 230.9562 and 120.0801 were observed in positive ion mode, indicating that “ SO_3 ” was added to the hydroxy group of ring A. Compound 14 was tentatively deduced as naringenin sulfate. The hypothesized fragmentation pathways of compound 14 is presented in Supplementary Figure S1.

Two terpenoid sulfate compounds (38 and 66) were tentatively identified. Compound 38 had an accurate mass $[M-H]^-$ ion at m/z 875.4055 with the formula $C_{42}H_{68}O_{17}S$, which was 80 Da more than that of soyasaponin III (52) ($C_{42}H_{68}O_{14}$, m/z 795.4553), indicating an exact “ SO_3 ” addition to soyasaponin III. It further produced 795.4521, 537.3282 and 457.3607, corresponding to the successive or simultaneous loss of SO_3 , a galactosyl moiety and a glucopyranosiduronic acid moiety, respectively. Therefore, Compound 38 was tentatively identified as soyasaponin III sulfate. Compound 66 produced an $[M-H]^-$ ion at m/z 537.3287 with the formula $C_{30}H_{50}O_6S$, and it further generated an ion at m/z 457.3633 consistent with soyasaponin I (51), soyasaponin III (52), soyasaponin II (53) and so on. Sulfate derivatives connected with feature compounds primarily come from esterification and dissociation of soyasapogenol B saponin. Therefore, Compound 66 was tentatively assigned as soyasapogenol B sulfate. The hypothesized fragmentation pathways of compounds 38 and 66 are shown in Supplementary Figure S2.

3.5. Possible transformation mechanism of components induced by sulfur fumigation

The transformation mechanism of terpenoid saponins was promoted by a hydrolysis reaction caused by SO_2 . According to the structural skeleton, the potential transformation pathways of terpenoid saponins could be classified into 3 types (oleanic acid, betulinic acid and soyasapogenol B), as shown in Fig. 4. For the oleanolic acid-type terpenoid saponins, oleanolic acid-3-O- α -L-rhamnopyranosyl-(1 \rightarrow 2)- β -D-galactopyranosyl-(1 \rightarrow 2)-glucuronopyranosyl-28-O- β -D-glucopyranoside (27) was first hydrolyzed with the cleavage of glycosidic bonds and transformed into oleanolic acid 3-O- α -L-rhamnopyranosyl-(1 \rightarrow 2)- β -D-galactopyranosyl-(1 \rightarrow 2)-glucuronopyranoside (56) under the promotion of SO_2 . Then, it was converted into ginsenoside Z-R1 (63, metabolite) and oleanolic acid (84) by successive hydrolysis reactions. Similarly, oleanolic acid 3-O- α -L-arabinopyranosyl-(1 \rightarrow 2)- α -L-rhamnopyranosyl-(1 \rightarrow 2)- β -D-galactopyranoside (57) was transformed into

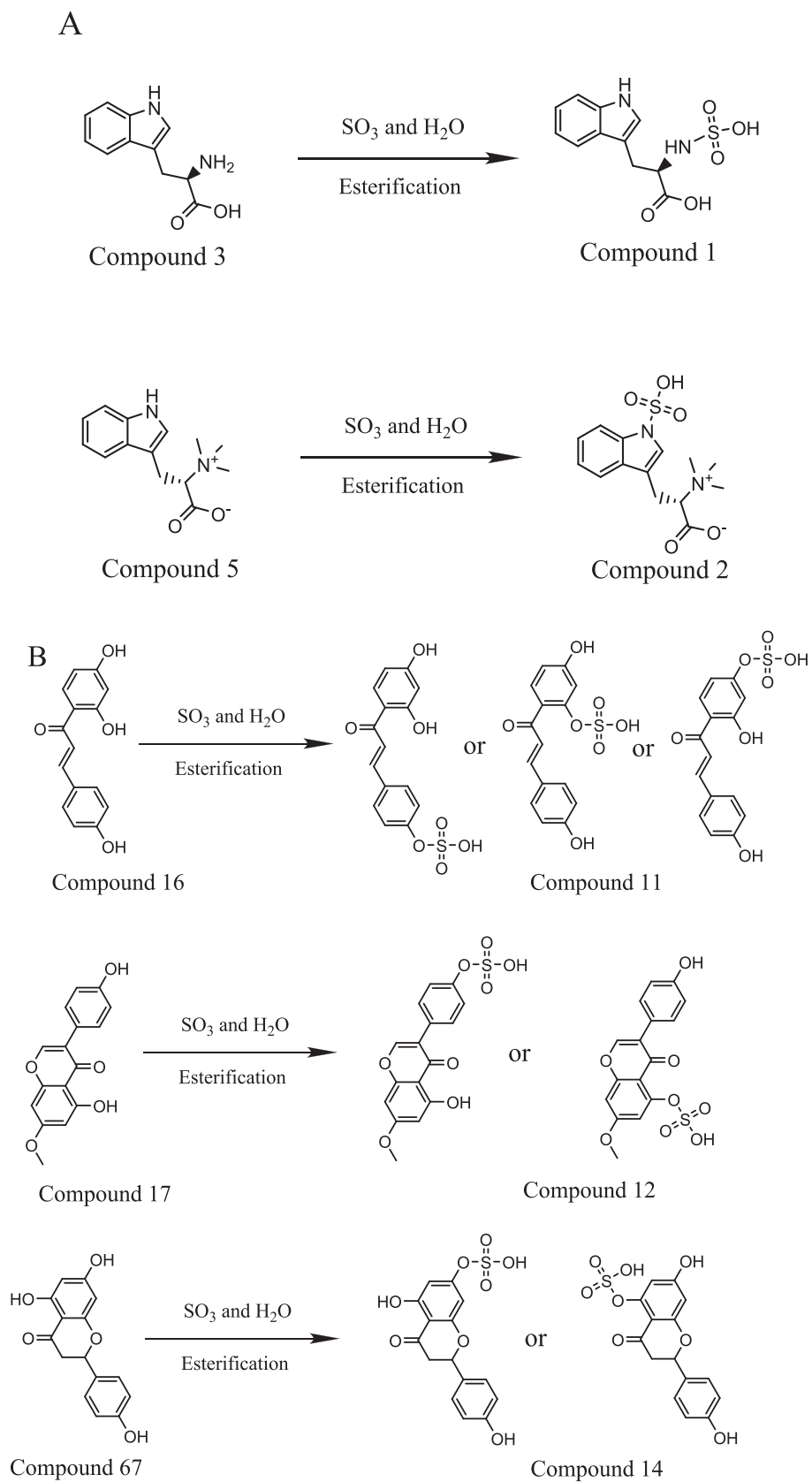


Fig. 5. A: The possible transformation mechanism of compounds 1 and 2; B: The possible transformation mechanism of compounds 11, 12 and 14; C: The possible transformation mechanism of compounds 38 and 66;

C

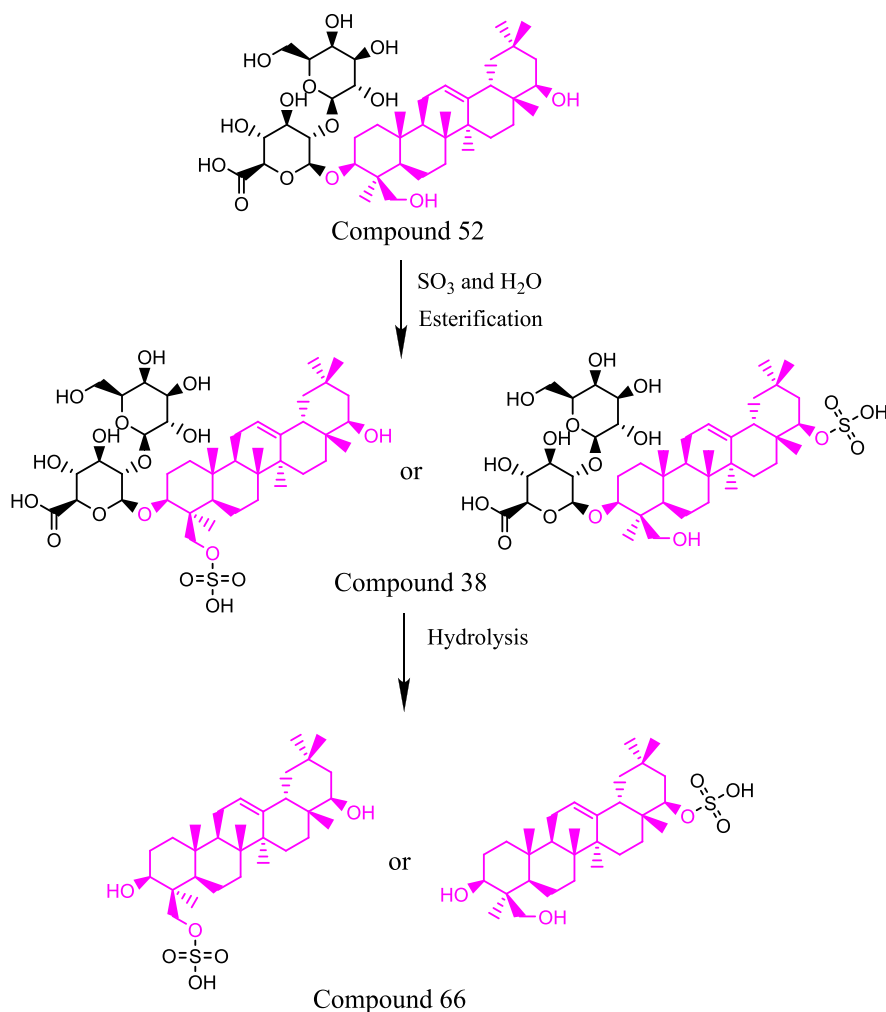


Fig. 5. (continued).

oleanolic acid 3-O- α -L-rhamnopyranosyl-(1 \rightarrow 2)- β -D-galactopyranoside (62) and oleanolic acid (84) by successive hydrolysis reactions under the promotion of SO₂. 3-O-Caffeoyloleanolic acid (76) was hydrolyzed to produce oleanolic acid (84). This could illustrate the phenomenon that peak 76 disappeared completely and peaks 62 and 84 increased significantly. In the case of the betulinic acid type, betulinic acid 3-O- α -L-rhamnopyranosyl-(1 \rightarrow 2)- β -D-galactopyranosyl-(1 \rightarrow 2)-glucuronopyranosyl-28-O- β -D-glucopyranoside (28), betulinic acid 3-O- α -L-arabinopyranosyl-(1 \rightarrow 2)- α -L-rhamnopyranosyl-(1 \rightarrow 2)- β -D-galactopyranoside (59) and pyracrenic acid (75) were hydrolyzed to generate betulinic acid (83). It could also explain the phenomenon that peak 75 nearly disappeared. The result of the soyasapogenol B type indicated that soyasapogenol B 3-O- α -L-rhamnopyranosyl-(1 \rightarrow 2)- β -D-galactopyranosyl-(1 \rightarrow 2)-glucuronopyranosyl-22-O- β -D-glucopyranoside (25) was deglycosylated to generate soyasaponin I (51); then, soyasaponin I could be converted to soyasaponin III (52). It was also found that soyasaponin VI (61) was transformed into soyasaponin I (51) or soyasaponin gamma (64, metabolite) by hydrolysis. Similarly, soyasaponin gamma (64, metabolite) was transformed into soyasaponin III (52) or 3-glucuronyl-22-DDMP soyasapogenol B (65, metabolite) under the promotion of SO₂. Taken together, terpenoid saponins could be converted into a large number of intermediate terpenoid saponins and their metabolites by hydrolysis reactions under the influence of the sulfur-fumigation process.

It was also necessary to explain the chemical transformation

mechanism of sulfate compounds that may be potentially harmful. From the present study, it was found that D-tryptophan (3) could be converted into D-tryptophan sulfate (1) during sulfur fumigation processing. Hypaphorine (5) is the characteristic precursor of hypaphorine sulfate (2). The findings agreed with the study that alkaloids were converted into their sulfate derivatives during the sulfur-fumigation process (Ma et al., 2014). The same change occurred for isoliquiritigenin (16), prunetin (17) and naringenin (67). The newly produced peaks appearing as isoliquiritigenin sulfate (11), prunetin sulfate (12) and naringenin sulfate (14) were generated by the addition of "SO₃" to different hydroxyl moieties in the flavonoid (He et al., 2018), while each sulfate derivative presents a single peak in the mass spectrum due to the isomers. In previous research, sulfur fumigation led to triterpene saponins transforming into their sulfate derivatives (Li et al., 2012; Kang et al., 2018; Zhang et al., 2021). In our work, we also found that sulfate derivatives of triterpene saponins could be generated during the sulfur fumigation process. Soyasaponin III (52) was partially converted to soyasaponin III sulfate (38) under sulfur fumigation, which caused a decrease in content. Soyasaponin III sulfate (38) may have two configurations, which are formed from the hydroxyl groups at position C-22 or C-24 of soyasaponin III (52). On the other hand, soyasaponin III sulfate lost sugar groups under acidic conditions and produced soyasapogenol B sulfate (66) during sulfur fumigation. These newly produced peaks indicated that sulfur fumigation can induce the chemical transformation of MSCP. The possible mechanisms deduced in the transformation mechanism of

sulfate compounds are shown in Fig. 5.

3.6. Exploring potential chemical markers based on multivariate statistical analysis

To distinguish the chemical profile differences between the NF-MSCP and SF-MSCP samples, unsupervised PCA was performed by SIMCA-P14.1. As shown in Fig. 6A, the result of the PCA score scatter plot showed that all samples were nearly classified into two groups. Except for sample SF-2, the other eight SF-MSCP samples (SF-1, SF-3 ~ 9) were gathered into the right of the $t[1]$ plot, while all the NF-MSCP samples (NF-1 ~ 10) were gathered to the left, illustrating that the chemical constituents and/or contents of components in MSCP remarkably changed during sulfur-fumigated processing.

Supervised OPLS-DA was further used to discriminate between NF-MSCP and SF-MSCP samples. The analysis indicated that the NF-MSCP

and SF-MSCP samples were obviously divided into two groups in OPLS-DA plots (Fig. 6B). An S-plot from OPLS-DA was further used to discover the potential chemical markers, and the points at either end of the S-plot together with the Variables of Importance in Projection (VIP) value ($VIP > 2.0$) generated from OPLS-DA were screened out as significant markers concerned with the difference between NF-MSCP and SF-MSCP samples (Kang et al., 2018; Zhang et al., 2021). From Fig. 6C, two points (a and b) on the lower left side and eight points (c, d, e, f, g, h, i and j) on the upper right of the S-type were considered important chemical markers. According to the base peak ion chromatogram, ten compounds were newly generated from sulfur-fumigated samples (peak 1: D-tryptophan sulfate; peak 2: hypaphorine sulfate; peak 11: isoliquiritigenin sulfate; peak 12: prunetin sulfate; peak 14: naringenin sulfate; peak 38: soyasaponin III sulfate; peak 63: ginsenoside Z-R1; peak 64: soyasaponin gamma; peak 65: lucuronyl-22-DDMP soyasapogenol B; peak 66: soyasapogenol B sulfate). Therefore, these ten compounds

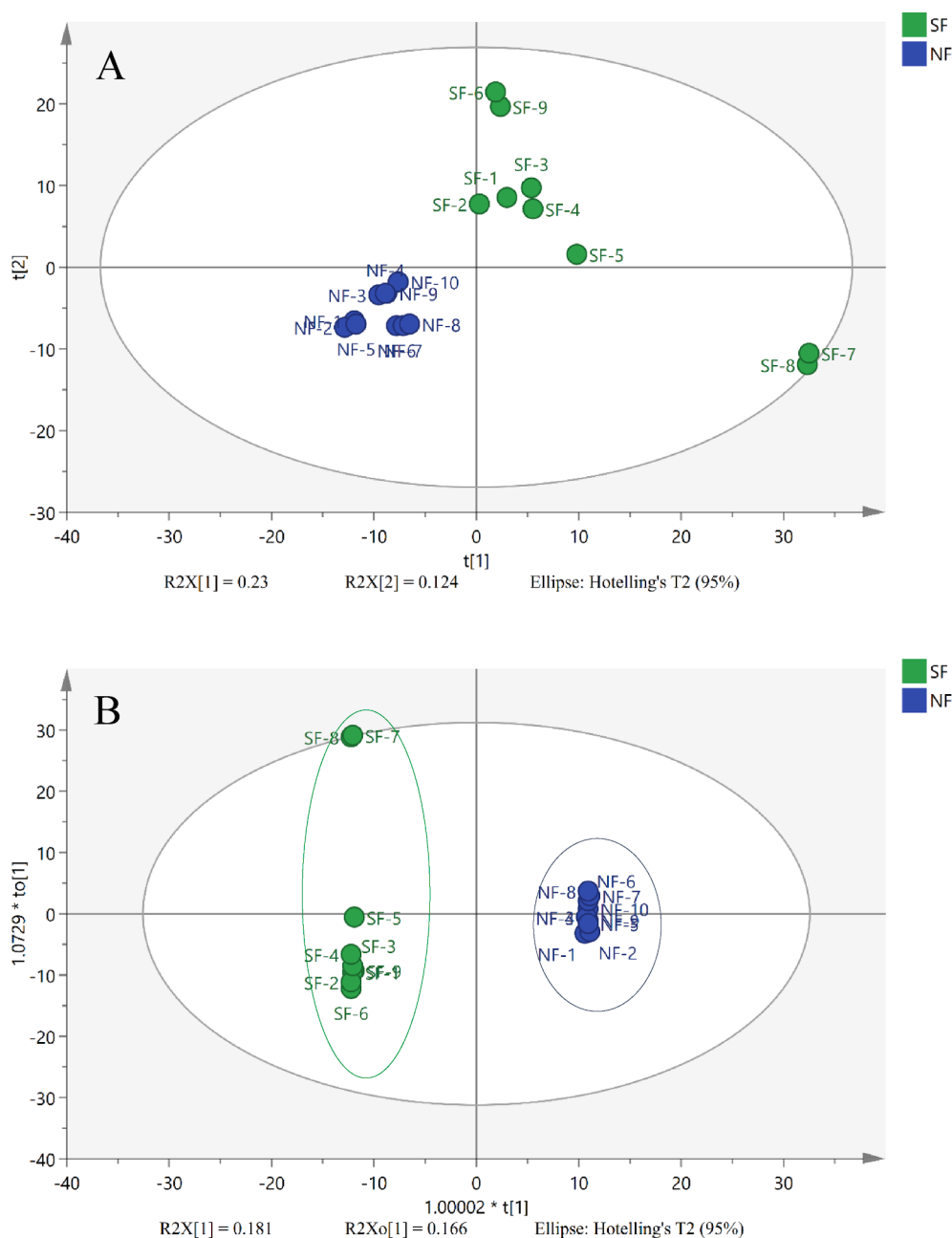


Fig. 6. A: PCA Scores plot of NF-MSCP and SF-MSCP samples; B: OPLS-DA Scores plot of NF-MSCP and SF-MSCP samples; C: S-Plot of NF-MSCP and SF-MSCP samples;

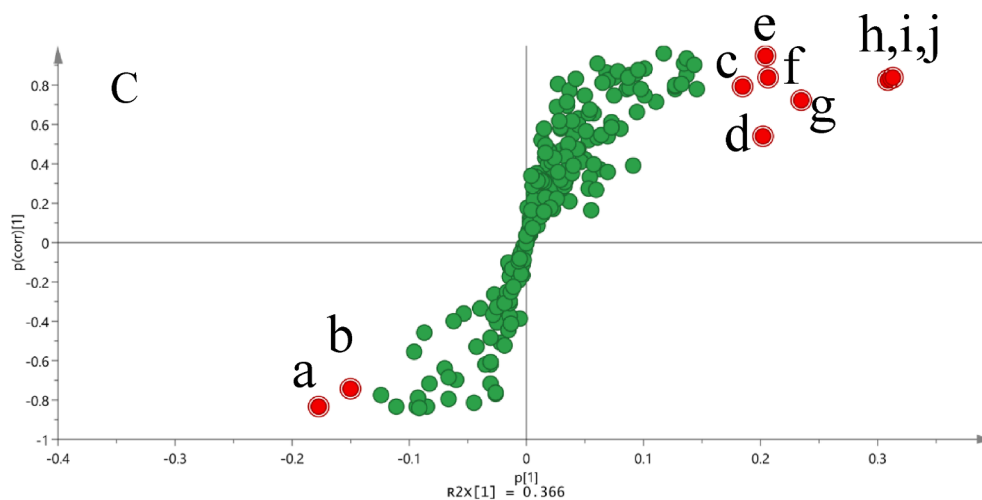


Fig. 6. (continued).

could be selected as potential markers to differentiate between the NF-MSCP and SF-MSCP samples.

3.7. Inspection of commercial MSCP samples

Ten markers were discovered distinguishing the NF-MSCP and SF-MSCP samples according to the above mechanism. The newly developed approach was used to inspect a total of 16 commercial MSCP samples obtained from the Yulin, Hehuachi, Qinzhou and Nanning markets in China. The results indicate that sulfur-containing compounds were found in 9 samples (Table 1), meaning that more than 50 % of commercial MSCP samples contained sulfur. It was also found that metabolites 63, 64 and 65 were detected in the above 9 sulfur-fumigated samples, but the metabolites were not detected in other commercial samples. It is obvious that the chemical constituents of MSCP can be transformed during the sulfur fumigation process.

3.8. Determination of sulfur residues

The sulfur residues in the samples are listed in Table 1. The sulfur contents of the sulfur-fumigated MSCP samples (SF-1 ~ 9) ranged from 120 to 630 mg/kg. Sulfur residues were also found in nine commercial MSCP samples, and the sulfur contents of the samples (S3, S4, S5, S7, S9, S12, S14, S15 and S16) were in the range of 100–310 mg/kg. It is important to note that there was much residual sulfur on the sample after sulfur fumigation, which might increase the potential incidence of toxicity. However, the bioactivities and toxicity of sulfur-fumigated MSCP need to be further studied.

4. Conclusions

Sulfur fumigation has been reported to cause chemical transformation and alter the original bioactive ingredients in herbs or their extracts, which could lead to changes in bioactivity and pharmacokinetics and even toxicity (Wigenstam, Elfsmark, Bucht, & Jonasson, 2016; Yuan et al., 2019; Shen et al., 2020). In this study, a novel UHPLC–QTOF–MS/MS approach based on chemical profiling and multivariate statistical analysis was established to discover chemical markers in SF-MSCP samples. Ten potential chemical markers was found in sulfur-fumigated samples, including 7 sulfur-containing compounds and 3 terpenoid metabolites. The new sulfated derivative was generated through esterification and/or addition of the original compound with SO₃ during the sulfur-fumigation process. The newly developed approach was successfully used to analyze sixteen commercial MSCP samples, nine of them which contained sulfur-containing compounds.

These sulfur residue contents of the SF-MSCP sample ranged from 100 to 310 mg/kg.

These research outcomes not only can be used to distinguish the NF-MSCP from SF-MSCP by chemical markers but also provide a chemical basis for further comprehensive investigating in-depth safety and functional evaluations of SF-MSCP.

Author contributions

This study was conceived by Zhifeng Zhang. Jianguang Zhang drafted the manuscript. Lili He conducted the UHPLC–QTOF–MS/MS analysis. Junjun Wang and Li Yang identified all the chemical compounds. Ming Chen determined the sulfur residues. Zichang Liang conducted the statistical analysis.

Declaration of competing interest

The authors declare that they have no known competing financial interests or personal relationships that could have influenced the work reported in this study.

Acknowledgment

This work was supported by the Sichuan Provincial Regional Innovation Cooperation Project, China (2023YFQ0084), the Fundamental Research Funds for the Central Universities, Southwest Minzu University, China (ZYN2023099) and the Technology Research and Development Project of Qinzhou Science and Technology Bureau, China (20198509).

Appendix A. Supplementary material

Supplementary data to this article can be found online at <https://doi.org/10.1016/j.arabjc.2023.105509>.

References

- Chen, Q.P., He, L.L., Mo, C.M., Zhang, Z.F., Long, H.R., Gu, X.Y., Wei, Y., 2018. Rapid evaluation of chemical consistency of artificially induced and natural Resina Draconis using ultra-performance liquid chromatography quadrupole-time-of-flight mass spectrometry-based chemical profiling. *Molecules* 23 (8), 1850–1855. <https://doi.org/10.3390/molecules23081850>.
- Chi, Z., Mo, Y.Y., Feng, S.S., Meng, M.W., Chen, S.Y., Huang, H.M., Su, Z.H., 2021. Urinary metabolomics study of anti-depressive mechanisms of *Milletia speciosa* Champ on rats with chronic unpredictable mild stress-induced depression. *J. Pharm. Biomed. Anal.* 205 (25), 114338 <https://doi.org/10.1016/j.jpba.2021.114338>.

- Chiang, T.C., Chang, H.M., 1982. Isolation and structural elucidation of some saponins from *Abrus cantoniensis*. *Planta Med.* 46 (9), 52–55. <https://doi.org/10.1055/s-2007-970019>.
- Chinese Pharmacopoeia Commission. (2020). Chinese Pharmacopoeia 2020 (Chinese Edition). China: Beijing.
- Fu, M.Q., Xiao, G.S., Xu, Y.J., Wu, J.J., Chen, Y.L., Qiu, S.X., 2016. Chemical constituents from roots of *Milletia speciosa*. *Chinese Herb. Med.* 8 (4), 385–389. [https://doi.org/10.1016/S1674-6384\(16\)60068-0](https://doi.org/10.1016/S1674-6384(16)60068-0).
- Ha, T.J., Lee, B.W., Park, K.H., Jeong, S.H., Kim, H., Ko, J., Lee, J.H., 2014. Rapid characterization and comparison of saponin profiles in the seeds of Korean Leguminous species using ultra performance liquid chromatography with photodiode array detector and electrospray ionisation/mass spectrometry (UPLC–PDA–ESI/MS) analysis. *Food Chem.* 146 (1), 270–277. <https://doi.org/10.1016/j.foodchem.2013.09.051>.
- He, L.L., Zhang, Z.F., Liu, Y., Chen, D.Q., Yuan, M.H., Dong, G.T., Yan, Z.G., 2018. Rapid discrimination of raw and sulfur-fumigated *Smilax glabra* based on chemical profiles by UHPLC-QTOF-MS/MS coupled with multivariate statistical analysis. *Food Res. Int.* 108, 226–236. <https://doi.org/10.1016/j.foodres.2018.03.047>.
- Huang, Z., Zeng, Y.J., Chen, X., Luo, S.Y., Pu, L., Li, F.Z., Lou, W., 2020. A novel polysaccharide from the roots of *Milletia Speciosa* Champ: preparation, structural characterization and immunomodulatory activity. *Int. J. Biol. Macromol.* 145, 547–557. <https://doi.org/10.1016/j.ijbiomac.2019.12.166>.
- Huang, Z., Zong, M.H., Long, W.Y., 2022. Effect of acetylation modification on the emulsifying and antioxidant properties of polysaccharide from *Milletia speciosa* Champ. *Food Hydrocoll.* 124, 107217 <https://doi.org/10.1016/j.foodhyd.2021.107217>.
- Jiang, X., Huang, L.F., Zheng, S.H., Chen, S.L., 2013. Sulfur fumigation, a better or worse choice in preservation of Traditional Chinese Medicine. *Phytomedicine* 20 (2), 97–105. <https://doi.org/10.1016/j.phymed.2012.09.030>.
- Jiang, J., Xiao, S.C., Yan, S., Zhang, J.X., Xu, X.M., 2020. The effects of sulfur fumigation processing on *Panax quinquefolii* Radix in chemical profile, immunoregulation and liver and kidney injury. *J. Ethnopharmacol.* 249, 112377 <https://doi.org/10.1016/j.jep.2019.112377>.
- Kang, C.Z., Zhao, D., Kang, L.P., Wang, S., Lv, C.G., Zhou, L., Guo, L.P., 2018. Elucidation of characteristic sulfur-fumigated markers and chemical transformation mechanism for quality control of *Achyranthes bidentata* blume using metabolome and sulfur dioxide residue analysis. *Front. Plant Sci.* 9, 790. <https://doi.org/10.3389/fpls.2018.00790>.
- Li, S.L., Shen, H., Zhu, L.Y., Xu, J., Jia, X.B., Zhang, H.M., Xu, H.X., 2012. Ultra-high-performance liquid chromatography-quadrupole/time of flight mass spectrometry based chemical profiling approach to rapidly reveal chemical transformation of sulfur-fumigated medicinal herbs, a case study on white ginseng. *J. Chromatogr. A* 1231, 31–45. <https://doi.org/10.1016/j.chroma.2012.01.083>.
- Ma, B., Kan, W.L.T., Zhu, H., Li, S.L., Lin, G., 2017. Sulfur fumigation reducing systemic exposure of ginsenosides and weakening immunomodulatory activity of ginseng. *J. Ethnopharmacol.* 195, 222–230. <https://doi.org/10.1016/j.jep.2016.11.023>.
- Ma, X.Q., Leung, A.K., Chan, C.L., Su, T., Li, W.D., Li, S.M., Yu, Z.L., 2014. UHPLC Q-TOF MS/MS analysis of the impact of sulfur fumigation on the chemical profile of *Codonopsis Radix* (Dangshen). *Analyst* 139 (2), 505–516. <https://doi.org/10.1039/c3an01561k>.
- Ma, X.B., Wu, Y.J., Li, Y., Huang, Y.F., Liu, Y., Luo, P., Zhang, Z.F., 2020. Rapid discrimination of *Notopterygium incisum* and *Notopterygium franchetii* based on characteristic compound profiles detected by UHPLC-QTOF-MS/MS coupled with multivariate analysis. *Phytochem. Anal.* 31 (3), 355–365. <https://doi.org/10.1002/pca.2902>.
- Massiot, G., Lavaud, C., Benkhald, M., Men-Olivier, L.L., 2004. Soyasaponin VI, A new maltol conjugate from alfalfa and soybean. *J. Nat. Prod.* 55 (9), 1339–1342. <https://doi.org/10.1021/np50087a031>.
- Shen, H., Zhang, L., Xu, J.D., Ding, Y.F., Zhou, J., Wu, J., Li, S.L., 2020. Effect of sulfur-fumigation process on ginseng: Metabolism and absorption evidences. *J. Ethnopharmacol.* 256, 112799 <https://doi.org/10.1016/j.jep.2020.112799>.
- Shi, H.M., Wen, J., Tu, P.F., 2006. Chemical constituents of *Abrus cantoniensis*. *Chinese Trad. Herb. Med.* 37 (11), 1610–1613. <https://doi.org/10.7501/j.issn.0253-2670.2006.11.2006011705>.
- Uchiyama, T., Furukawa, M., Isobe, S., Makino, M., Akiyama, T., Koyama, T., Fujimoto, Y., 2003. New olenae-type triterpene saponins from *Milletia speciosa*. *Heterocycles* 60 (3), 655–661.
- Wang, X.H., Xie, P.S., Lam, C.W.K., Yan, Y.Z., Yu, Q.Y., 2009. Study of the destructive effect to inherent quality of *Angelicae dahuricae radix* (Baizhi) by sulfur-fumigated process using chromatographic fingerprinting analysis. *J. Pharm. Biomed. Anal.* 49 (5), 1221–1225. <https://doi.org/10.1016/j.jpba.2009.03.009>.
- Wang, M.Y., Zhang, M., Yang, Q., Wang, Q.L., Ma, B.K., Li, Z.Y., Cheng, W., Wang, Z.N., 2021. Metabolomic profiling of *M. speciosa* champ at different growth stages. *Food Chem.* 376, 131941 <https://doi.org/10.1016/j.foodchem.2021.131941>.
- Wigenstam, E., Elfsmark, L., Bucht, A., Jonasson, S., 2016. Inhaled sulfur dioxide causes pulmonary and systemic inflammation leading to fibrotic respiratory disease in a rat model of chemical-induced lung injury. *Toxicology* 368–369. <https://doi.org/10.1016/j.tox.2016.08.018>.
- Yin, T., Tu, G.Z., Zhang, Q.Y., Wang, B., Zhao, Y.Y., 2008. Three new phenolic glycosides from the caulis of *Milletia speciosa*. *Magn. Reson. Chem.* 46 (4), 387–391. <https://doi.org/10.1002/mrc.2189>.
- Yuan, M.H., Yan, Z.G., Liu, Y., Chen, D.Q., Yang, Z.J., He, L.L., Zhang, Z.F., 2019. Chemical profiles, antioxidant activity and acute toxicity of raw and sulfur-fumigated *Smilax glabrae* Rhizoma. *J. Ethnopharmacol.* 234, 76–84. <https://doi.org/10.1016/j.jep.2019.01.026>.
- Zhang, M., Cui, C.H., Lin, Y.D., Cai, J.Y., 2021. Ameliorating effect on glycolipid metabolism and chemical profile of *Milletia speciosa* champ. extract. *J. Ethnopharmacol.* 279 (114360) <https://doi.org/10.1016/j.jep.2021.114360>.
- Zhang, Y.N., Wang, B., Zhao, P.H., He, F., Xiao, W., Zhu, J.B., Ding, Y., 2021. A comprehensive evaluation protocol for sulfur fumigation of ginseng using UPLC-Q-TOF-MS/MS and multivariate statistical analysis. *Lwt-Food Sci. Technol.* 145, 111293 <https://doi.org/10.1016/j.lwt.2021.111293>.
- Zhang, J.G., Wang, J.J., Wang, Y., Chen, M., Shi, X.M., Zhou, X.P., Zhang, Z.F., 2022. Phytochemistry and antioxidant activities of the rhizome and radix of *Milletia speciosa* based on UHPLC-Q-exactive orbitrap-MS. *Molecules* 27 (21), 7398. <https://doi.org/10.3390/molecules27217398>.
- Zhao, X.N., Liang, J.L., Chen, H.B., Liang, Y.E., Guo, H.Z., Su, Z.R., Zhang, X.J., 2015. Anti-fatigue and antioxidant activity of the polysaccharides isolated from *Milletia speciosa* Champ. *Nutrients* 7 (10), 8657–8669. <https://doi.org/10.3390/nu7105422>.
- Zhao, Z.Y., Liu, P.H., Ma, S.S., Wang, S.L., Li, A., Liu, J.G., Wang, M., 2017. Botanical characteristics, chemical and nutritional composition and pharmacological and toxicological effects of medicinal and edible plant *Milletia speciosa* Champ. *Food Sci.* 38 (9), 293–306.
- Zhou, S.S., Hu, J.W., Kong, M., Xu, J.D., Shen, H., Chen, H.B., Li, S.L., 2019. Less SO₂ residue may not indicate higher quality, better efficacy and weaker toxicity of sulfur-fumigated herbs: Ginseng, a pilot study. *J. Hazard. Mater.* 364, 376–387. <https://doi.org/10.1016/j.jhazmat.2018.10.038>.